nature chemistry

ARTICLES

PUBLISHED ONLINE: 4 SEPTEMBER 2011 | DOI: 10.1038/NCHEM.1127

Self-reproduction of supramolecular giant vesicles combined with the amplification of encapsulated DNA

Kensuke Kurihara[1], Mieko Tamura[1], Koh-ichiroh Shohda[2,3], Taro Toyota[1,3], Kentaro Suzuki[1,3] and Tadashi Sugawara[1,3]*

The construction of a protocell from a materials point of view is important in understanding the origin of life. Both self-reproduction of a compartment and self-replication of an informational substance have been studied extensively, but these processes have typically been carried out independently, rather than linked to one another. Here, we demonstrate the amplification of DNA (encapsulated guest) within a self-reproducible cationic giant vesicle (host). With the addition of a vesicular membrane precursor, we observe the growth and spontaneous division of the giant vesicles, accompanied by distribution of the DNA to the daughter giant vesicles. In particular, amplification of the DNA accelerated the division of the giant vesicles. This means that self-replication of an informational substance has been linked to self-reproduction of a compartment through the interplay between polyanionic DNA and the cationic vesicular membrane. Our self-reproducing giant vesicle system therefore represents a step forward in the construction of an advanced model protocell.

The exploration of the origin of life is one of the most challenging scientific endeavours of this century and is being pursued using a variety of different approaches[1–3]. Model protocells in particular (defined as hypothetical pre-biological precursors of cells[4,5]) are expected to play a significant role in advancing our understanding[6–8]. In an article entitled 'Synthesizing life', Szostak *et al.*[9] identify the three critical components of a model protocell as being an informational substance[10] (such as RNA or DNA), a catalyst[11] (for example, an enzyme) and a compartment[12] (such as a vesicle). They also stress that the model protocell should self-reproduce the compartment and self-replicate the informational substance.

One approach to the construction of a model protocell is to use prebiotic materials such as fatty acids[13,14] and nucleotides[15,16]. The synthesis of oligonucleotides in a vesicle has also been extensively studied[17–20]. Thus far, however, self-replication of an informational substance (RNA or DNA) in a compartment and self-reproduction of the compartment (vesicle) have occurred independently. The second approach, known as a semi-synthetic approach[1,21,22], is based on the molecular assembly of biochemical components such as enzymes[23], DNA genes[24] and RNA[25] that have been purified from a living cell. In a pioneering investigation, Oberholzer *et al.*[26] constructed a model protocell consisting of RNA, a viral RNA polymerase (Qβ-replicase), and an oleate/oleic acid small vesicle (diameter < 100 nm). The third approach, called a supramolecular approach[27–30], targets a model protocell in which the key issue is how to realize self-reproductive dynamics of artificial lipids that interact with amplifying informational substances (DNA or RNA) in a vesicle. For example, we have recently reported the construction of self-reproducing giant vesicles (GVs, diameter >1 μm) composed of an artificial cationic membrane molecule and its precursor[31–35]. In these studies, a membrane precursor was first added to a dispersion of GVs bearing an amphiphilic catalyst. The precursor was converted to membrane molecules within the GV, which subsequently grew and divided into daughter GVs. In other experiments, we have also achieved polymerase chain reaction (PCR) amplification of a 1.2 kb DNA fragment within a phospholipid GV[36].

In this Article, we describe the construction of an advanced model protocell that links the process of self-replication of the informational substance with the self-reproduction of the vesicle compartment, as shown in Fig. 1a,b. We selected DNA as the informational substance because it is more robust than RNA. Including a cationic membrane molecule in the vesicular membranes enabled us to induce electrostatic interactions between the positively charged membrane of the GV (host) and the amplified polyanionic DNA (encapsulated guest). It was found that the GVs in which DNA is successfully amplified by PCR grow and divide notably faster than those in which DNA amplification is not observed. Our findings suggest that the processes of DNA amplification and the growth and division of GVs are chemically linked in our model protocell (Fig. 1). Our model protocell is therefore, albeit at a fundamental level, relevant to the chemoton model proposed by Gánti[37].

Results and discussion

Self-reproducing GVs with encapsulated DNA. For a model protocell to be achieved, the daughter GVs obtained by the self-reproducing process of an original GV must contain the informational substance (here, DNA). This means that the informational substance must be amplified before the GV divides. To amplify the DNA in the self-reproducing GV, we used PCR, because it requires DNA polymerase as the sole protein. For successful amplification of DNA, GVs must have sufficient space for an enzymatic reaction, and must be resistant to a highly ionic medium and high temperature. In addition, the surface charge of the membrane should not interfere with the activity of enzymes in the GV.

The addition of a zwitterionic phospholipid (1-palmitoyl-2-oleoyl-*sn*-glycero-3-phosphocholine, POPC) to our previously

[1]Department of Basic Science, Graduate School of Arts and Sciences, University of Tokyo, 3-8-1 Komaba, Meguro-ku, Tokyo 153-8902, Japan, [2]Department of Life Sciences, Graduate School of Arts and Sciences, University of Tokyo, 3-8-1 Komaba, Meguro-ku, Tokyo 153-8902, Japan, [3]Research Center of Life Science as Complex Systems, University of Tokyo, 3-8-1 Komaba, Meguro-ku, Tokyo 153-8902, Japan. *e-mail: suga@pentacle.c.u-tokyo.ac.jp

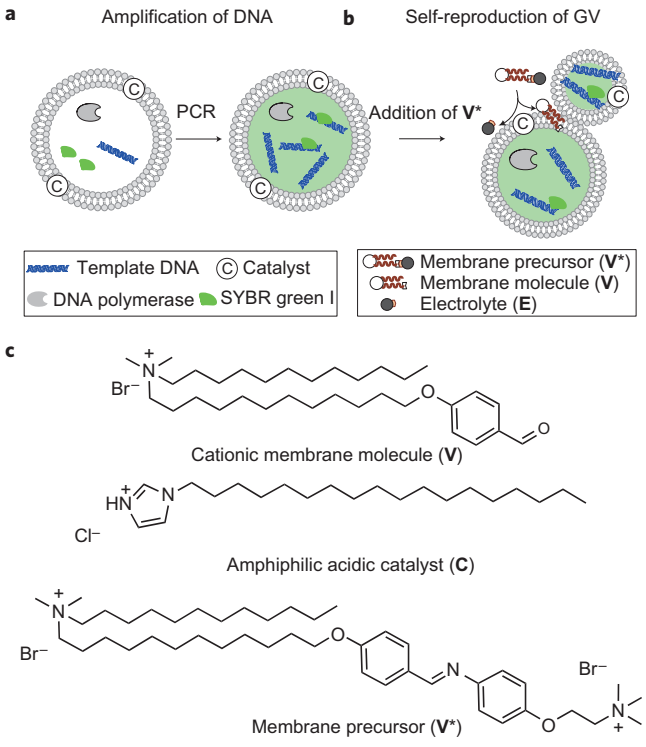

Figure 1 | Schematic representation of the chemical link between amplification of DNA and self-reproduction of GVs. a, Amplification of DNA within a GV. An aqueous dispersion of GVs containing PCR reagents was prepared using a film-swelling method with a buffered solution containing template DNA, primers, fluorescent tag SYBR Green I, deoxynucleoside triphosphates, DNA polymerase and Mg^{2+}. **b**, Vesicular self-reproduction induced by adding membrane precursor **V***. Addition of **V*** produces membrane molecules and electrolytes through hydrolysis assisted by an amphiphilic catalyst. Adhesion of the amplified DNA to the inner leaflet accelerates vesicular growth and division. **c**, Chemical structures of membrane molecule **V**, amphiphile catalyst **C** and membrane precursor **V***.

studied myelin-type GVs composed of a positively charged membrane molecule **V**[33–35] (Fig. 1c) enabled the construction of a hollow GV with an inner cavity filled with water. An anionic phospholipid (1-palmitoyl-2-oleoyl-*sn*-glycero-3-phosphoglycerol, POPG) was added in an amount equimolar to the cationic **V** to reduce the surface charge. The addition of POPG was also effective in producing GVs that were stable at high temperatures and also under conditions of high ionic strength (Supplementary Section S3 and Figs S1 and S2). The optimized molar ratio of our hybrid membrane, including the amphiphilic acidic catalyst **C** with an imidazolium head group, was 6:2:2:1 [POPC:POPG:**V**:**C**] (Supplementary Table S1).

To prepare the GVs, the thin lipid films made of the amphiphiles described above were swollen with a PCR solution containing a 1,229-base pair (bp) template DNA (Supplementary Table S2a). We added deoxyribonuclease I (DNase I) to the bulk water phase to digest template DNA remaining outside of the GVs so that amplification of DNA would only occur within the GV (Supplementary Table S2b). We noticed that the extrusion method (see Methods) reorganized initially formed GVs of a myelin-type GV to GV with a sufficient inner volume. Thus we adopted this method to produce GVs within which enzymatic reactions were able to proceed. By observing samples under a microscope, we confirmed the presence of GVs with a diameter of ~10 μm. Because GVs with diameters of 10 μm statistically contain 30 DNA templates under these conditions[36], DNA amplification in these GVs is expected to proceed smoothly, although the validity of the statistical estimation is sometimes argued[38].

Amplification of DNA encapsulated within the GVs. Amplification of the DNA was conducted within the GVs using two-step thermal cycling conditions[36], and detected by fluorescence emitted from a double-stranded DNA–SYBR Green I complex (dsDNA–SG complex)[39] when SG was introduced within the GVs. Intense fluorescence was observed only after the amplification process (Fig. 2a). We confirmed, using gel electrophoresis, that the length of the amplified DNA was the same as that of the template DNA (Supplementary Section S4 and Fig. S3).

We used flow cytometric analysis to estimate the ratio of GVs with encapsulated amplified DNA (DNA-amplified GVs) to the total number of GVs (Fig. 2b, Supplementary Section S5). The shape of the histogram of fluorescence intensity before PCR is symmetrical, with a maximum frequency centred at 60 along the fluorescence intensity axis (arbitrary units) (Fig. 2b). After PCR, the histogram is asymmetrical, and deconvolution of the histogram revealed the appearance of a new group of GVs displaying a maximum frequency at a fluorescence intensity of ~200. Population analysis revealed that the DNA-amplified GVs represented ~20% of the total number of GVs. Judging from the increase in fluorescence intensity after PCR, it was estimated that the amount of DNA increased by a factor of $\sim 1 \times 10^2$ for 10-μm-sized giant vesicles, which was reasonable when the molar ratio ($\sim 1 \times 10^6$) of deoxyribonucleoside triphosphates (dNTPs) to 1,229-bp template DNA was taken into account. Oberholzer *et al.* described amplification using a dispersion of small to large vesicles (SV/LVs, where LVs have average diameters of <200 nm)[18], but the percentage of SV/LV with encapsulated amplified DNA (DNA-amplified SV/LV) was less than 0.1% owing to the low probability of encapsulation of the DNA template (369 bp) into SV/LVs. The ratio of DNA-amplified GV to the total number of GVs was crucially higher than that of the DNA-amplified SV/LV reported in the previous work. This difference is most likely the result of differences in the efficiency of entrapment of the PCR reagents owing to the large inner volume of GVs compared with SV/LVs[18].

Self-reproduction of DNA-amplified GVs. We observed the DNA-amplified GVs performing the self-reproduction process following the addition of the bolaamphiphilic[40] membrane precursor **V*** (Fig. 1c) using differential interference contrast microscopy and fluorescence microscopy at a real-time speed (Fig. 2c, see Methods). The growth and morphological changes of the GVs occurred within 4 min of the addition of **V***, and serial divisions of DNA-amplified GVs produced multiple GVs within 15 min. The daughter GVs were almost the same size as the mother GV (Supplementary Section S6 and Movie). Moreover, the effective partitioning of the amplified DNA to the daughter GVs was achieved owing to the presence of cationic membrane molecules, as revealed by the fluorescence microscopic images of the daughter GVs (Fig. 2c, bottom). To clarify the role of amplified DNA in GV self-reproduction, we performed two negative control experiments. When they were not subject to any thermal cycle, the GVs rarely divided within the 2 h time period of the experiment (Supplementary Section S7, Control Experiment A). When GVs were subjected to thermal cycling without DNA polymerase, 9 of 100 GVs underwent division only once within the same time period (Supplementary Section S7, Control Experiment B). Taken together, these findings suggest that amplified DNA is essential for inducing rapid growth and division of the GVs.

If equivolume division of a GV occurs with a sufficient amount of DNA, two daughter GVs will be produced that each contain half of the original amount of DNA. This explains the decrease in the

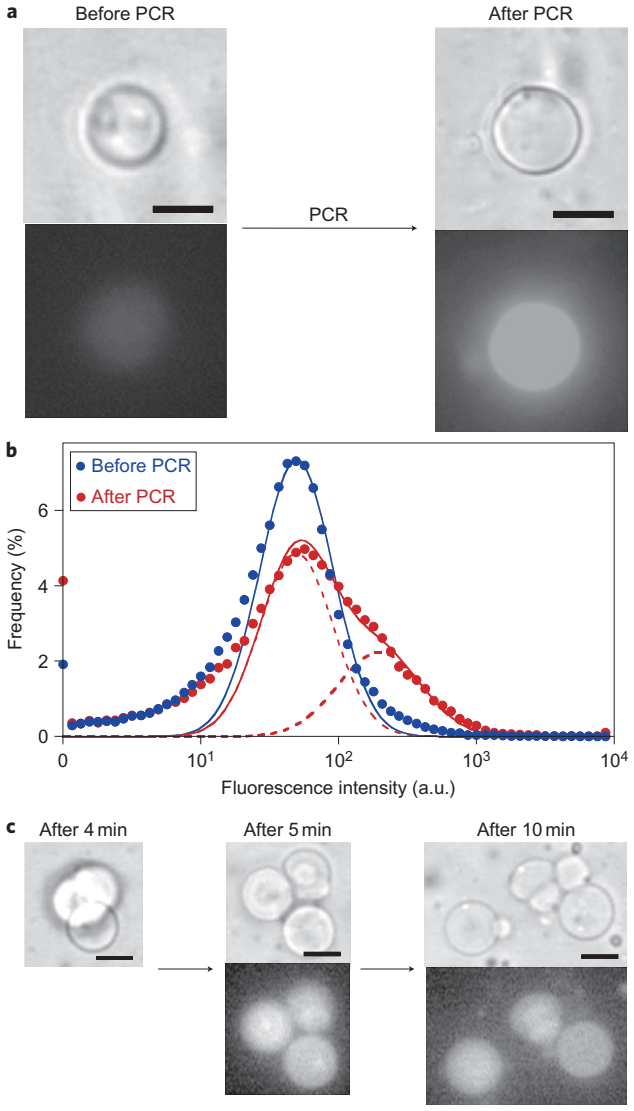

Figure 2 | Amplification of DNA inside GVs and growth-and-division of DNA-amplified GVs. a, Microscopic images of a DNA-amplified GV before and after DNA amplification: (top) differential interference contrast microscopic images; (bottom) fluorescence microscopic images visualized due to the dsDNA–SG complex inside the GV. Scale bars, 10 μm. Samples were obtained by extruding suspended swollen GVs 20 times through a polycarbonate membrane filter (diameter, 12 μm). **b**, Histograms of fluorescence intensity (constructed using flow cytometry) of GVs before and after DNA amplification. The fluorescence histogram shifted to a higher intensity after amplification compared to before. **c**, Real-time observation of morphological changes of DNA-amplified GVs after addition of $\mathbf{V}^*$. Original GVs began to grow and divide 4 min after adding $\mathbf{V}^*$. Complete division into four GVs occurred at 5.5 min, and separation occurred at 7 min (top panels). Partition of DNA was detected using fluorescence microscopy (bottom panels). Scale bars, 10 μm.

number of GVs with a sufficient amount of DNA, as revealed by flow cytometric analysis (Supplementary Section S8 and Fig. S6). Under the microscope, we unambiguously observed that the partition of DNA associated with the GV self-reproduction is a ubiquitous event after the addition of the membrane precursor.

Influence of amplified DNA on GV division. The frequency of GV division in the presence of amplified DNA was notably higher than that of GVs in the absence of amplified DNA. A control experiment revealed that the effect of the temperature of thermal cycling on the division of GV is negligible (Supplementary Section S7, Control Experiment B). We therefore hypothesize that the division of GVs is driven by DNA adhering to the inner membrane surface. A straightforward control experiment would be the preparation of GVs containing different amounts of DNA in an inner water pool, and comparing the rate of growth and division caused by the addition of $\mathbf{V}^*$. However, when a thin film of lipids was swollen by a buffered solution of DNA, the cationic membrane and polyanionic DNA formed a lipoplex[41] and no GVs were formed. Alternatively, the amount of DNA of DNA-amplified GVs is expected to vary according to the number of thermal cycles. We expect that the frequency of GV division will also vary, thus providing support for the dependence of GV division on amplified DNA.

We therefore investigated the effect of the number of thermal cycles, and hence of the amount of amplified DNA, on the frequency of GV division by using a flow cytometric study in which the GV membrane was stained with an amphiphilic fluorescent probe (Rhod-DOPE) (Fig. 3a,b). Because the ratio of Rhod-DOPE to lipids was only 0.01 mol%, the effect of the probe on the size and lamellarity of the GVs and on the amplified DNA within the GVs should be negligible. We postulated that the amount of fluorescent probe in vesicular membranes per GV must decrease according to the number of divisions. Provided that the lamellarity of the GVs is consistent, the size should be proportional to the number of membrane molecules and thus the amount of fluorescent probe. Then the decrease in fluorescence intensity of membrane-stained GVs must be related to the division frequency of DNA-amplified GV, as schematically shown in Fig. 3a. Because we traced the self-reproduction dynamics of large GVs under an optical microscope, we focused on the decrease in the number of ~10-μm-sized large GVs, the fluorescence intensity of which was 1×10^3 (arbitrary unit) on the basis of calibration using filtering experiments[34,35]. This selection is reasonable, because the lamellarity of 10-μm-sized large GVs is reduced for the enzymatic activity, and the smaller GVs with high lamellarity pass through the mesh of the filter. As a result, effective GV divisions were observed only for large GVs.

Time courses for the number of GVs showing a fluorescence intensity of 1×10^3 after the addition of $\mathbf{V}^*$ are plotted in Fig. 3c, where plots A, B and C show data for GVs subjected to 20, 15 and 10 thermal cycles, respectively. Plot A shows that with 20 thermal cycles, the number of such GVs decreased rapidly. Plot C shows that after 10 thermal cycles, 20% of the GVs disappeared rapidly, and the remaining 80% were unchanged. Plot B shows that when the GVs were subjected to 15 thermal cycles, ~80% of them decreased gradually, and the decay of the remaining 20% was even slower. It is claimed that enzymatic performance within a GV depends on the GV having sufficient inner volume. If the lamellarity of the GV membrane is low and if sufficient PCR reagents are encapsulated within the inner cavity, one can expect that the efficiency of amplification is optimal and a sufficient amount of DNA is produced in some of the GVs, even after 10 thermal cycles. If the template DNA and polymerase become encapsulated into different compartments in a GV, it is possible that the efficiency of amplification is decreased. Because the pseudo-first-order rate constants of GVs subjected to 20 and 0 thermal cycles are $k_{20} = 3 \times 10^{-1}$ min^{-1} and $k_0 = 5 \times 10^{-3}$ min^{-1}, respectively, the ratio of decay rates is ~60:1 for the two types of GVs. This ratio is in good agreement with the frequency of division determined by optical microscopy. GVs subjected to 20 thermal cycles divided within 2–3 min, whereas GVs that were not subjected to any thermal cycle divided once in 120 min.

Mechanism underlying GV growth and division. Our findings suggest that the growth-and-division process of the GVs is driven

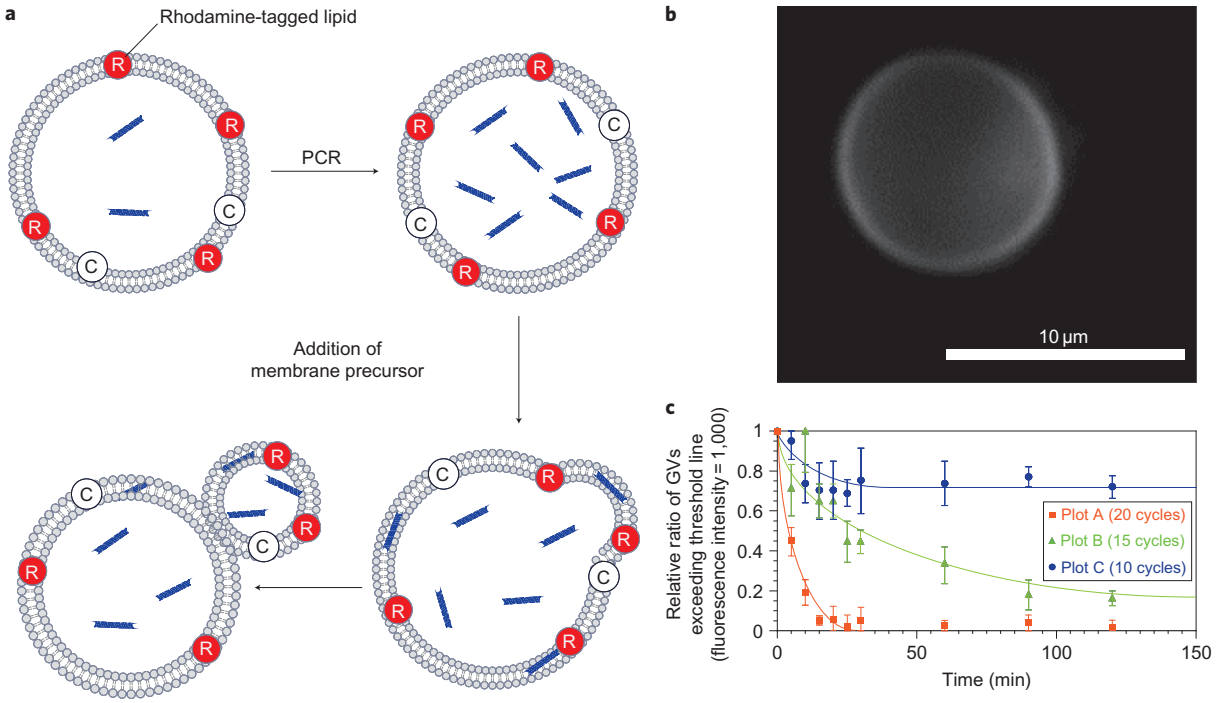

Figure 3 | Influence of the amount of amplified DNA on the division frequency of DNA-amplified GVs stained by rhodamine-tagged lipids. a, Self-reproduction of GVs with membranes stained with rhodamine-tagged lipids. **b**, Fluorescence image of GV with rhodamine-tagged lipids. Rhodamine-stained GV was prepared by mixing stock $CHCl_3$ solutions of POPC (10 mM, 60 μl), POPG (10 mM, 20 μl), **V** (10 mM, 20 μl), **C** (10 mM, 10 μl) and Rhod-DOPE (1 mM, 1 μl) in a test tube. The initial concentration of Rhod-DOPE added to the lipid mixture was 0.01 mol%. **c**, Decay kinetics for the number of GVs with a fluorescence intensity of 1×10^3 (arbitrary unit) after DNA amplification following addition of $\mathbf{V}^*$. Plots A, B and C present the numbers of remaining GVs with a fluorescence intensity of 1×10^3 after 20, 15 and 10 thermal cycles, respectively. GVs with a fluorescence intensity of 1×10^3 were chosen because of the negligible contribution of divided GVs with a fluorescence intensity higher than 1×10^3. The pseudo-first-order decay rate constants were evaluated to be $k_0 = 5 \times 10^{-5}$ min^{-1}, $k_{10} = 2 \times 10^{-2}$ min^{-1}, $k_{15} = 3 \times 10^{-2}$ min^{-1} and $k_{20} = 3 \times 10^{-1}$ m^{-1} for plots A, B and C, respectively, where k_i denotes the initial rate constant for GVs with i thermal cycles.

by the presence of amplified DNA. Angelova and co-workers[42,43] reported that rapid fission of positively charged GVs occurs when they are exposed to a DNA solution because of the strong interaction between these oppositely charged substances. In contrast, we found that the amount of DNA within the GV cavity increased with PCR thermal cycling when starting with a small amount of template DNA (~30 molecules in a 10-μm-sized GV)[36]. We assume that some of the DNA molecules, the amount of which increased during thermal cycling, adhere to the inner surface of the vesicular membrane (Fig. 4a,b, right). It appears that DNA adhesion occurs because of the accumulation of cationic **V** molecules within the inner leaflet of the lipid bilayer and because these molecules cover the DNA (Fig. 4b,c). The existence of buried dsDNA in the outer vesicular membrane was confirmed in a fluorescence microscopic image showing that not only the inside but also the periphery of the DNA-amplified GV fluoresced owing to the presence of dsDNA–SYBR Green I complex (Supplementary Section S9, Fig. S7). This observation is supported by a previous study in which polyanionic DNA was shown to form a lipoplex with cationic membranes[41]. The accumulation of **V** around DNA, which occurred in the inner leaflet of the outer membrane, results in an imbalance in the number of membrane molecules between the inner and outer leaflets. This imbalance might lead to pre-organization for the budding-type deformation of GV (Fig. 4d).

The membrane precursor $\mathbf{V}^*$ can incorporate within the vesicular membrane from either side of the polar head groups: from the head group of the membrane side (*Hm*) or from the head group of the electrolyte side (*He*) (Fig. 4a). This means that when the membrane molecule **V** is formed from $\mathbf{V}^*$ in the vicinity of the buried DNA, the number of **V** in both the inner and outer leaflets is increased without flip-flop motions[33–35], depending on the direction of its head group. $\mathbf{V}^*$ can penetrate the inner membranes unless it is hydrolysed by **C** in the outer membrane. This characteristic behaviour of $\mathbf{V}^*$ is advantageous for the rapid growth and division of DNA-amplified GVs into daughter GVs.

We revealed that GV division induced by cationic $\mathbf{V}^*$ is very slow in the absence of amplified encapsulated DNA (Supplementary Section S7). Figure 4e shows a GV without amplified DNA. In this case, dissolved $\mathbf{V}^*$ in the vesicular membrane may diffuse freely into the outer water phase before being hydrolysed by **C**. In contrast, in the case of a DNA-amplified GV, some of the amplified DNA is buried between two leaflets of the outer membrane. Hence the chance for cationic $\mathbf{V}^*$ to be trapped by the DNA becomes high in the vicinity of DNA compared with the rest of the outer membrane (Fig. 4d). As a result, the membrane precursor $\mathbf{V}^*$ is efficiently hydrolysed to produce the membrane molecule **V** by the catalytic activity of **C**, which diffuses laterally in the vesicular membrane, although the proposed mechanism for the assistance of DNA in the growth and division of GV is still at a speculative stage.

It is interesting to compare the mechanism of GV division and partitioning of amplified DNA in our GV-based model protocell with that of a prokaryotic cell. In a prokaryotic cell such as *E. coli*, specific nucleotide sequences (*oriCs*) on the chromosome bind to the cell membrane early in the replication of the chromosome, assisted by a protein complex[44]. Thereafter, the cell membrane between the two connected points elongates and becomes squeezed, and the genomic DNA becomes equally distributed between the two daughter cells. Thus, in a prokaryotic cell, specific proteins mediate the separation of DNA and the division of the cellular membrane. In our protocell, the

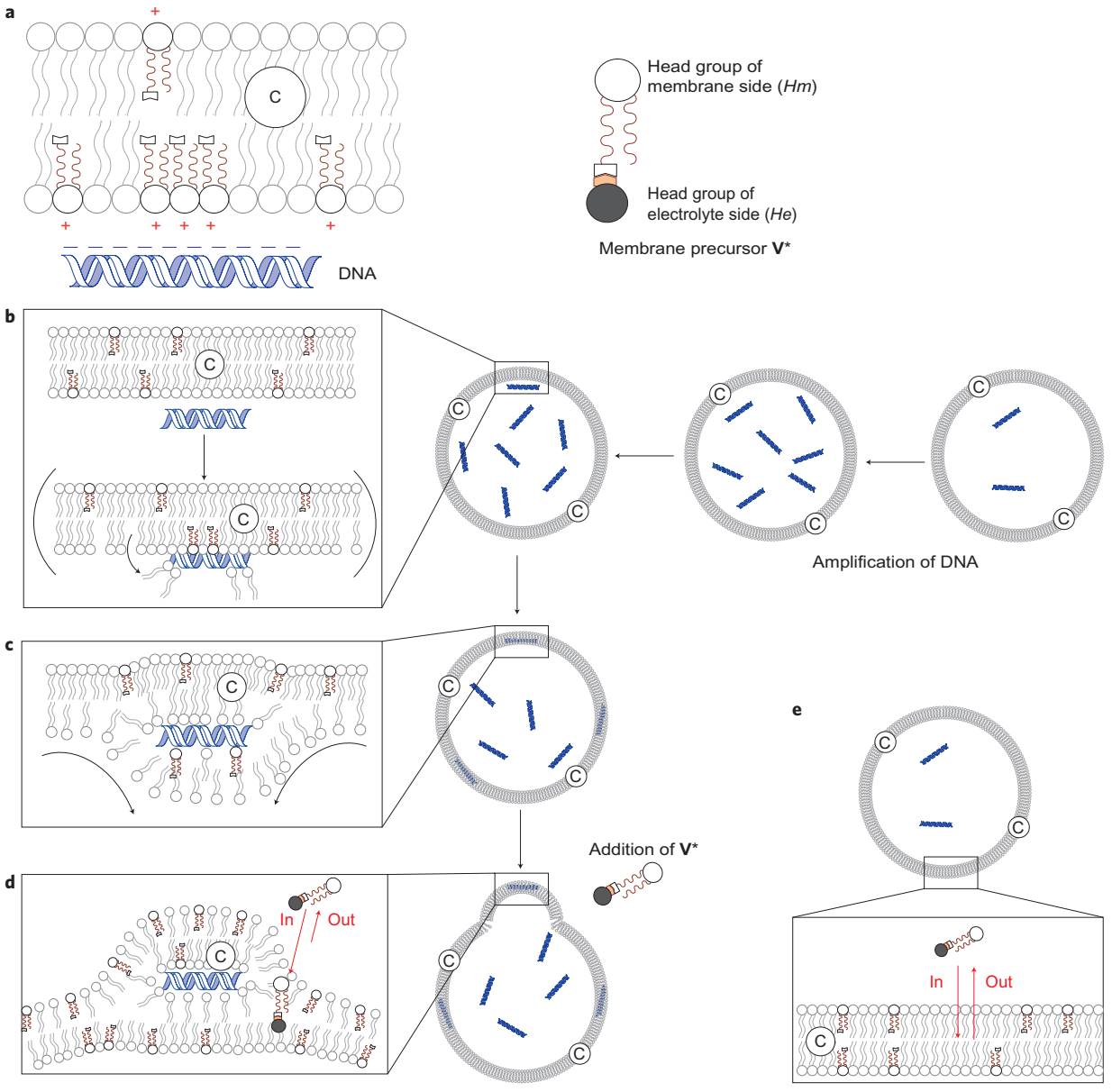

Figure 4 | Effect of amplified encapsulated DNA on the dynamics of self-reproducing GVs. a, DNA adhesion onto the inner surface of the outer vesicular membrane (side view along the DNA chain), including an acidic amphiphilic catalyst **C**. A schematic structure of bolaamphiphilic membrane precursor $\mathbf{V}^*$ with two polar head groups (*Hm* and *He*) is also depicted: polar groups are represented by red + and blue − signs. **b**, DNA adhesion onto the membrane (side view). Cationic **V** covers the surface of polyanionic DNA. **c**, DNA is fully covered with cationic **V** and buried between the inner and outer leaflets, causing an imbalance in the number of **V** molecules between the inner and outer leaflets. **d**, Bolaamphiphilic membrane precursor $\mathbf{V}^*$ is captured by the buried DNA and then hydrolysed by catalyst **C**. **V** molecules increase the number of outer or inner leaflets of the vesicular membranes, depending on the direction of dissolution (*Hm*-top or *He*-top) of $\mathbf{V}^*$. **e**, In contrast, if $\mathbf{V}^*$ dissolves in a vesicular membrane containing no amplified DNA, $\mathbf{V}^*$ is likely to diffuse to the outer water phase without being hydrolysed by catalyst **C**.

amplified DNA is partitioned by the collaborative dynamics of DNA, cationic membrane molecules **V** and bolaamphiphilic membrane precursor $\mathbf{V}^*$, and not by specific proteins. Natural cells replicate their genomes by physically connecting the DNA with the membrane through the mediation of proteins. In contrast, our model protocell shows that a similar but non-protein-mediated DNA–membrane interaction operates and can drive GV division. The result suggests that prebiotic processes used such natural interactions, which were later strengthened or better controlled with proteins.

Conclusions

In our self-reproducing GVs, amplified DNA interacts with the vesicular membrane and induces a morphological change in the host GV. These processes not only lead to the growth and division of GVs, but also to the partitioning of the amplified DNA into the daughter GVs. Therefore, in this supramolecular approach, amplification of an information substance (DNA) and self-reproduction of a compartment (GV) are linked chemically.

The drawback of the present system is that self-reproduction is limited. This is because the composition of the membrane molecules gradually changes as the number of self-reproducing vesicles increases: the percentage of phospholipids decreases and this is accompanied by an increase in the level of cationic artificial membrane molecules. If phospholipids and nucleotides could be conveyed into our protocell with a molecular transportation system, such as vesicular fusion[45,46], then our self-reproducing vesicular

system should continue dividing, and this might eventually lead to the development of protocells to which natural selection could be applied.

Methods

PCR solution. The PCR solution (1 ml) contained water (600 μl), PCR buffer solution (10× KOD Plus buffer, 100 μl), $MgSO_{4(aq)}$ (25 mM, 40 μl), poly(ethylene glycol)$_{aq}$ (12.5 wt%, 80 μl), dNTP mix (2 mM each dNTP in TE buffer, 80 μl), 24-mer primer (10 μM, 30 μl), 22-mer primer (10 μM, 30 μl), 1,229-bp DNA template (10 nM, 10 μl), 1 × SYBR Green I dye (commercial product diluted 10,000× in TE buffer, 10 μl) and KOD Plus polymerase (1 U μl^{-1}, 20 μl). The TE buffer was a dispersion of 10 mM Tris-HCl buffer containing 1 mM EDTA (Tris = 2-amino-2-hydroxymethylpropane-1,3-diol; EDTA = ethylenediaminetetraacetic acid).

Preparation of giant vesicles. Stock solutions of POPC (10 mM, 60 μl), POPG (10 mM, 20 μl), **V** (10 mM, 20 μl) and **C** (10 mM, 10 μl) in $CHCl_3$ were mixed in a test tube. The solvent was evaporated under a flow of nitrogen. Under these conditions, thin lipid films formed on the inner surface of the test tube. The remaining $CHCl_3$ in the glass tube was removed under reduced pressure over a period of 2 h. Addition of the PCR solution (1 ml) to this lipid film, followed by vortex mixing (5–10 s), resulted in the formation of a GV dispersion with a total lipid concentration of 2 mM. This GV dispersion was passed 20 times through a syringe with a 12 μm pore membrane filter. The GVs containing the template DNA were subjected to amplification in a thermal cycler (iCycler, Bio-Rad Laboratories Japan).

Protocol of thermal cycling. The GV dispersion was treated with a thermal cycler under the following thermal conditions: 94 °C for 2 min (94 °C for 15 s and 68 °C for 90 s) for 20 cycles (the lid of the PCR tube was heated to 105 °C). After the thermal cycles had been performed, the dispersion was slowly cooled to room temperature.

Microscopic observation. A specimen for microscopic observations was prepared as follows. The vesicular dispersion was placed between two plates of cover glass with a spacer (17 × 28 mm, 0.3 mm thick; Frame Seal Chamber, MJ Research) adhered to the cover-glass plates. Difference interference contrast and fluorescence microscopic images of the GVs were obtained with an optical microscope (IX 70, Olympus) equipped with a ×20 objective lens and a filter set (λ_{ex}, 460–490 nm; λ_{em}, 510–550 nm). To observe vesicular dynamics, a dispersion of the membrane precursor $\mathbf{V}^*$ (2 mM) was prepared by dissolving powdered $\mathbf{V}^*$ in a PCR buffer solution with sonication for 5 min. This dispersion was passed through a polycarbonate filter (pore size, 200 nm). The resulting dispersion of $\mathbf{V}^*$ was mixed with an equimolar dispersion of GVs containing amplified DNA before observation under a microscope.

Detection of amplified DNA. Polyacrylamide gel electrophoresis of GVs containing amplified DNA was performed after lipids and enzymes were removed from the buffered solution containing the PCR product by treatment with TE buffer solution (150 μl) saturated with phenol-chloroform-iso-amylalcohol (25:24:1, v/v/v) (Supplementary Section S4).

Flow cytometry. Population analysis of DNA-amplified GVs was conducted using a fluorescence-activated flow cytometer (EPICS ALTRA Hyper Sort Type3, Beckman Coulter), equipped with an Ar^+ laser (excitation at 488 nm) to assay the GVs containing amplified DNA. Population analysis of GVs stained with Rhod-DOPE was conducted with the flow cytometer used to assay the GVs containing amplified DNA. Stock $CHCl_3$ solutions of POPC (10 mM, 60 μl), POPG (10 mM, 20 μl), **V** (10 mM, 20 μl), **C** (10 mM, 10 μl) and Rhod-DOPE (1 mM, 1 μl) were mixed in a test tube. Rhod-DOPE was incorporated into the GVs at an initial mole percentage of 0.01 mol%. The remaining $CHCl_3$ in the tube was removed under reduced pressure over a period of 2 h.

Received 2 March 2011; accepted 26 July 2011; published online 4 September 2011

References

1. Luisi, P. L. *The Emergence of Life: From Chemical Origins to Synthetic Biology* (Cambridge Univ. Press, 2006).
2. Gardner, P. M., Winzer, K. & Davis, B. D. Sugar synthesis in a protocellular model leads to a cell signaling response in bacteria. *Nature Chem.* **1,** 377–383 (2009).
3. Gibson, D. G. *et al.* Creation of bacterial cell controlled by a chemically synthesized genome. *Science* **329,** 52–56 (2010).
4. Walde, P. Building artificial cells and protocell models: experimental approaches with lipid vesicles. *Bioessays* **32,** 296–303 (2010).
5. Luisi, P. L., Ferri, F. & Stano, P. Approaches to semi-synthetic minimal cells: a review. *Naturwissenschaften* **93,** 1–13 (2006).
6. Stano, P. & Luisi, P. L. Achievement and open questions in the self-reproduction of vesicles and synthetic minimal cells. *Chem. Commun.* **46,** 3639–3653 (2010).
7. Fleischaker, G. R., Colonna, S. & Luisi, P. L. (eds) *Self-Production of Supramolecular Structures: From Synthetic Structures to Models of Minimal Living Systems* (Kluwer, 1994).
8. Hanczyc, M. M., Fujikawa, S. M. & Szostak, J. W. Experimental models of primitive cellular compartments: encapsulation, growth, and division. *Science* **302,** 618–622 (2003).
9. Szostak, J. W., Bartel, D. P. & Luisi P. L. Synthesizing life. *Nature* **409,** 387–390 (2001).
10. Gesteland, R. F., Cech, T. R. & Atkins, J. F. (eds) *The RNA World* 3rd edn (Cold Spring Harbor Laboratory Press, 2005).
11. Lee, D. H., Granja, J. R., Martinez, J. A., Severin, K. & Ghadiri, M. R. A self-replicating peptide. *Nature* **382,** 525–528 (1996).
12. Segré, D., Ben-Eli, D., Deamer, D. & Lancet, D. The lipid world. *Orig. Life Evol. Biosph.* **1–2,** 119–145 (2001).
13. Mansy, S. S., Schrum, J. P., Krishnamurthy, M., Tobé S., Treco, D. A. & Szostak, J. W. Template-directed synthesis of a genetic polymer in a model protocell. *Nature* **454,** 122–125 (2008).
14. Mansy, S. S. & Szostak, J. W. Thermostability of model protocell membranes. *Proc. Natl. Acad. Sci. USA* **105,** 13351–13355 (2008).
15. Powner, M. W., Gerland, B. & Sutherland, J. D. Synthesis of activated pyrimidine ribonucleotides in prebiotically plausible condition. *Nature* **459,** 239–242 (2009).
16. Powner, M. W., Sutherland, J. D. & Szostak, J. W. Chemoselective multicomponent one-pot assembly of purine precursors in water. *J. Am. Chem. Soc.* **132,** 16677–16688 (2010).
17. Oberholzer, T., Albrizio, M. & Luisi, P. L. Polymerase chain reaction in liposome. *Chem. Biol.* **2,** 677–682 (1995).
18. Chakrabarti, A. C., Breaker, R. R., Joyce, G. F. & Deamer, D. W. Production of RNA by a polymerase protein encapsulated within phospholipid vesicles. *J. Mol. Evol.* **39,** 555–559 (1994).
19. Walde, P., Goto, A., Monnard, P-A., Wessicken, M. & Luisi, P. L. Oparin's reactions revisited: enzymatic synthesis of poly(adenylic acid) in micelles and self-reproducing vesicles. *J. Am. Chem. Soc.* **116,** 7541–7547 (1994).
20. Zepik, H. H. & Walde, P. Achievements and challenges in generating protocell models. *ChemBioChem* **9,** 2771–2772 (2008).
21. Chiarabelli, C., Stano, P. & Luisi, P. L. Chemical approaches to synthetic biology. *Curr. Opin. Biotechnol.* **20,** 492–497 (2009).
22. Kuruma, Y., Stano, P., Ueda, T. & Luisi, P. L. A synthetic biology approach to the construction of membrane proteins in semi-synthetic minimal cells. *Biochim. Biophys. Acta.* **1788,** 567–574 (2009).
23. Sunami, T., Hosoda, K., Suzuki, H., Matsuura, T. & Yomo, T. Cellular compartment model for exploring the effect of the lipidic membrane on the kinetics of encapsulated biochemical reactions. *Langmuir* **26,** 8544–8551 (2010).
24. Nomura, S. M. *et al.* Gene expression within cell-sized lipid vesicles. *ChemBioChem.* **4,** 1172–1175 (2003).
25. Kita, H. *et al.* Replication of genetic information with self-encoded replicase in liposomes. *ChemBioChem.* **9,** 2403–2410 (2008).
26. Oberholzer, T., Wick, R., Luisi, P. L. & Biebricher, C. K. Enzymatic RNA replication in self-reproducing vesicles: an approach to a minimal cell. *Biochem. Biophys. Res. Comm.* **207,** 250–257 (1995).
27. Atwood, J. L., Davies, J. E. D., Macnicol, D. D., Vögtle, F. & Lehn, J-M. (eds) *Comprehensive Supramolecular Chemistry* (Pergamon, 1996).
28. Lehn, J-M. *Supramolecular Chemistry: Concepts and Perspectives* (Wiley-VCH, 1995).
29. Ariga, K. & Kunitake, T. *Supramolecular Chemistry—Fundamentals and Applications* (Springer, 2006).
30. Muraoka, T., Kinbara, K. & Aida, T. Mechanical twisting of a guest by a photoresponsive host. *Nature* **440,** 512–515 (2006).
31. Suzuki, K., Toyota, T., Takakura, K. & Sugawara, T. Sparkling morphological changes and spontaneous movements of self-assemblies in water induced by chemical reactions. *Chem. Lett.* **38,** 1010–1015 (2009).
32. Takakura, K., Toyota, T. & Sugawara, T. A novel system of self-reproducing giant vesicles. *J. Am. Chem. Soc.* **125,** 8134–8140 (2003).
33. Takakura, K. & Sugawara, T. Membrane dynamics of a myelin-like giant multilamellar vesicle applicable to a self-reproducing system. *Langmuir* **20,** 3832–3834 (2004).
34. Toyota, T. *et al.* Population study of sizes and components of self-reproducing giant multilamellar vesicles. *Langmuir* **24,** 3037–3044 (2008).
35. Kurihara, K., Takakura, K., Suzuki, K., Toyota, T. & Sugawara, T. Cell-sorting of robust self-reproducing giant vesicles tolerant to a highly ionic medium. *Soft Matter* **6,** 1888–1891 (2010).
36. Shohda, K. *et al.* Compartment size dependence of performance of polymerase chain reaction inside giant vesicle. *Soft Matter* **7,** 3750–3753 (2011).
37. Gánti, T. *The Principles of Life* (Oxford Univ. Press, 2003).
38. de Souza, T. P., Stano, P. & Luisi, P. L. The minimal size of liposome-based model cells brings about remarkably enhanced entrapment and protein synthesis. *ChemBioChem* **11,** 1056–1063 (2010).
39. Zipper, H., Brunner, H., Bernhagen, J. & Vitzthum, F. Investigations on DNA intercalation and surface binding by SYBR Green I, its structure determination and methodological implications. *Nucleic Acids Res.* **32,** e103 (2004).

40. Fuhrhop, J-H. & Wang, T. Bolaamphiphiles. *Chem. Rev.* **104,** 2901–2937 (2004).
41. Rädler, J. O., Koltover, I., Salditt, T., & Safinya, C. R. Structure of DNA–cationic liposome complexes: DNA intercalation in multilamellar membranes in distinct interhelical packing regimes. *Science* **275,** 810–814 (1997).
42. Angelova, M. I. & Tsoneva, I. Interactions of DNA with giant liposomes. *Chem. Phys. Lipids* **101,** 123–137 (1999).
43. Angelova, M. I., Histova, N. & Tsoneva, I. DNA-induced endocytosis upon local microinjection to giant unilamellar cationic vesicles. *Eur. Biophys. J.* **28,** 142–150 (1999).
44. Ogden, G. B., Pratt, M. J. & Schaechter, M. The replicative origin of the *E. coli* chromosome binds to cell membranes only when hemimethylated. *Cell* **54,** 127–135 (1988).
45. Maru, N., Shohda, K. & Sugawara, T. Successive fusion of vesicles aggregated by DNA duplex formation in the presence of Triton X-100. *Chem. Lett.* **37,** 340–341 (2008).
46. Pantos, A., Tsiourvas, D., Paleos, C. M. & Nounesis, G. Enhanced drug transport from unilamellar liposomes induced by molecular recognition of their lipid membranes. *Langmuir* **21,** 6696–6702 (2005).

Acknowledgements

The authors acknowledge financial support from KAKENHI (Grant-in Aid for Scientific Research) for Priority Area 'Soft Matter Physics' (area no. 463) from the Ministry of Education, Culture, Sports, Science, and Technology of Japan. The authors also thank M.M. Hanczyc for helpful discussions.

Author contributions

T.S., K.K. and K.Su. conceived and designed the experiments. K.K. performed experiments. M.T. contributed the protocol. K.Su. contributed analysis. T.T. and K.Sh. contributed discussion of the data. T.S. wrote the paper. All authors discussed the results and commented on the manuscript.

Additional information

The authors declare no competing financial interests. Supplementary information and chemical compound information accompany this paper at www.nature.com/naturechemistry. Reprints and permission information is available online at http://www.nature.com/reprints. Correspondence and requests for materials should be addressed to T.S.